



**Simplified Modeling of Tropospheric Ozone Formation Considering Alternative Fuels Using
Modelagem Simplificada da Formação de Ozônio
Troposférico Considerando o Uso de Combustíveis Alternativos.**

Leonardo Aragão Ferreira da Silva¹;
Jesus Salvador Pérez Guerrero² & Luiz Claudio Gomes Pimentel^{1,3}

¹Universidade Federal do Rio de Janeiro, Centro de Tecnologia, COPPE,
Departamento de Engenharia Mecânica, Bloco G, 21.945-970, Rio de Janeiro/RJ, Brasil

²Comissão Nacional de Energia Nuclear, Rua General Severiano, 90, 22.290-901, Rio de Janeiro/RJ, Brasil

³Universidade Federal do Rio de Janeiro, IGEO, CCMN, Departamento de Meteorologia,
Av. Athos da Silveira Ramos, 274 – Bloco H, Sala H2-014 – Cidade Universitária, 21.941-916,
Ilha do Fundão – Rio de Janeiro/RJ, Brasil

E-mails: aragao@lamma.ufrj.br; jperez@cnen.gov.br; pimentel65@gmail.com

Recebido em: 07/09/2014 Aprovado: 12/12/2014

DOI: http://dx.doi.org/10.11137/2014_2_151_160

Abstract

Brazilian cities have been constantly exposed to air quality episodes of high ozone concentrations (O_3). Known for not being emitted directly into the environment, O_3 is a result of several chemical reactions of other pollutants emitted to atmosphere. The growth of vehicle fleet and government incentives for using alternative fuels like ethanol and Compressed Natural Gas (CNG) are changing the Brazilian Metropolitan Areas in terms of acetaldehyde and formaldehyde emissions, Volatile Organic Compounds (VOC's) present in the atmosphere and known to act on the kinetics of ozone. Driven by high concentrations of tropospheric ozone in urban/industry centers and its implications for environment and population health, the target of this work is understand the kinetics of ozone formation through the creation of a mathematical model in FORTRAN 90, describing a system of coupled ordinary differential equations able to represent a simplified mechanism of photochemical reactions in the Brazilian Metropolitan Area. Evaluating the concentration results of each pollutant were possible to observe the precursor's influence on tropospheric ozone formation, which seasons were more conducive to this one and which are the influences of weather conditions on formation of photochemical smog.

Keywords: tropospheric ozone; alternative fuels; VOC

Resumo

Nas últimas décadas diversas metrópoles brasileiras vêm sofrendo constantemente com eventos relacionados à qualidade do ar, a exemplo do Smog Fotoquímico, fenômeno caracterizado pelos altos níveis de concentração de ozônio (O_3) na baixa atmosfera. No entanto, sabe-se que este poluente não é emitido diretamente para o ambiente, o O_3 é fruto de diversas reações químicas que ocorrem na atmosfera na presença de outros poluentes. O crescimento da frota veicular e os incentivos do governo ao uso de combustíveis alternativos, como o álcool e o GNV, fizeram com que as grandes cidades do país registrassem um aumento nas concentrações de espécies como o formaldeído que, até então, não despertavam preocupações. Este poluente é um dos Compostos Orgânicos Voláteis (COV's) presentes na atmosfera, e estes compostos também são conhecidos por atuarem na cinética de formação do ozônio. Motivados pelos altos níveis de concentração de ozônio troposférico em centros urbano/industriais e suas implicações à saúde da população e do meio ambiente, buscamos neste trabalho entender a cinética de formação do ozônio através da criação de um modelo matemático computacional em linguagem FORTRAN 90, descrito por um sistema de equações diferenciais ordinárias acopladas, representando de forma simplificada os mecanismos de reações fotoquímicas da atmosfera. Em nossos resultados conseguimos observar como os poluentes precursores influenciam no processo de formação do ozônio na troposfera, quais as estações do ano mais propícias a este processo e quais influências das condições meteorológicas na formação do principal poluente do Smog Fotoquímico.

Palavras-chave: ozônio troposférico; combustíveis alternativos; COV

1 Introduction

During the last years Brazilian cities has been exposed to air quality episodes like photochemical smog, a phenomenon characterized by high concentrations of ozone (O_3) in lower atmosphere. However, this pollutant is not emitted directly into the environment. O_3 is a result of several chemical reactions of other pollutants emitted to atmosphere by biogenic and anthropogenic sources. Identify and estimate concentrations of these background pollutants are the biggest issues on ozone problem.

In 2005, the sector of transports was responsible for 21% of all energy consumed in Brazil, which have 85% based on petroleum resources. Behind this was the dependence on foreign oil, since that 50% of consumed oil in Brazil was imported. Thus economic impacts added to concerns about air quality encouraged the government to explore the use of alternative fuels to Brazilian fleet (Correa & Arbilla, 2005). The options were invest on Compressed Natural Gas (CNG) and reactivate the incentives for ethanol use, both based on economic reasons. Today, Brazil is the world's largest producer of bioethanol (and lower cost) with an established industry for over two decades. This, due a group of factors such as the large area available to sugar cane planting (main raw material), climatic and soil conditions favorable to production and all infrastructure built over the years. Nevertheless, the main result is the price of ethanol 50% cheaper than gasoline. The national program for use of pure ethanol (titled PRO-ÁLCOOL) and gasoline with 22% ethanol begins in 1979. In early 90's, several political crises led levels of bioethanol production to decreases considerably due the lack of planning for periods between sugar cane harvests, affecting drastically the production of new alcohol-fueled cars. In 1998, the government increased the percentage of ethanol in gasoline to 24% and the use of pure ethanol increased again (Martins *et al.*, 2007).

The growth of vehicle fleet and government incentives for using alternative fuels like ethanol and CNG has changed the air quality standards in Brazilian Metropolitan Areas. A few field-based studies have linked air pollution concerns with burning ethanol in Brazilian fleet (Grosjean *et al.*, 1998; Correa *et al.*, 2003; Fornaro & Gutz, 2003; Assunção *et al.*, 2005; Anderson, 2009).

At first, monitoring results pointed increases on ozone concentration, leading to investigate the background pollutants. Analyzing the fleet, vehicles moved by gasoline have high emission

of carbon monoxide (CO) and nitrogen oxides (NOx), both ozone precursors. The warning about vehicles moved by alcohol is the elevated emission of aldehydes, mainly acetaldehyde (CH_3CHO). To vehicles using CNG, preliminary studies shows high emission of aldehydes too, but with formaldehyde (HCHO) featured (Arbilla & Oliveira, 1999). Both HCHO and CH_3CHO acts at ozone formation and the relation between them indicate the contribution of each fuel. Literature results show that, in metropolitan areas, formaldehyde is almost always the predominant aldehyde emitted by automobiles and the acetaldehyde/formaldehyde ratio is always lesser than unit. Several studies analyzed exhaust characteristics of ethanol vehicles (Gaffney & Marley, 1990, 2009; Knapp *et al.*, 1998; MacLean & Lave, 2000; He *et al.*, 2003; Graham *et al.*, 2008; Wallner *et al.*, 2009). In contrast, experimental results for Brazilian cities showed acetaldehyde/formaldehyde ratios equal or higher than unit. This behavior was attributed to the use of hydrated ethanol and gasohol (gasoline with 24% of ethanol) as fuels (Nguyen *et al.*, 2001; Tanner *et al.*, 1988).

Another modeling study for urban areas like Los Angeles (U.S.A.), that uses ethanol 85% (E85) as alternative fuel, also suggests high levels of ozone due increased HCHO and CH_3CHO concentrations. This studying was conducted considering a reaction system with over 13,500 kinetic and photolysis reactions and 4,600 inorganic and organic species of the Master Chemical Mechanism (MCM), version 3.1, showing that even to the most complex models the problem of ozone associated with acetaldehyde and formaldehyde persists (Ginnebaugh *et al.*, 2010; Ginnebaugh & Jacobson, 2012).

Given the circumstances and the importance of discuss about photochemical smog modeling, the first aim of this study is develop a mathematical model able to representing a simplified kinetics of atmospheric photochemical reactions. Using this model, secondary objectives are understand the tropospheric ozone formation and relations with new vehicle fleet profile of Brazilian cities, that use alternative fuels such as ethanol and Compressed Natural Gas.

2 Problem Formulation

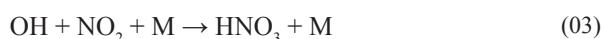
2.1 Atmospheric Chemical Reaction System

The ozone is a secondary pollutant derived from chemical reactions involving other pollutants. In this case, the main classes of precursors are

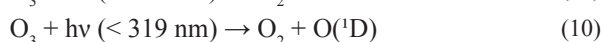
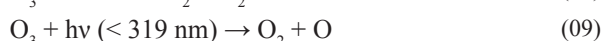
Nitrogen Oxides (NO_x) and Volatile Organic Compounds (VOC's). However, the ozone formation process begins on reaction of organic molecules with hydroxyl radical (OH), a free radical which does not react with major constituents of atmospheric air (N₂, O₂, CO₂ and H₂O). When Nitrogen Monoxide (NO) is available, HO₂ performs its most important reaction in the troposphere, providing OH to the system and entering a key component of ozone cycle, nitrogen dioxide (NO₂). The biggest part of NO_x emissions in the troposphere are at NO form. The other component, NO₂, is treated as secondary pollutant. Average concentrations of NO_x oscillate between 5 and 20 ppb in urban environments, 10 and 100 ppt in remote regions and approximately 1 ppb in rural areas (Seinfeld & Pandis, 2006).



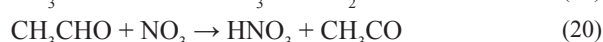
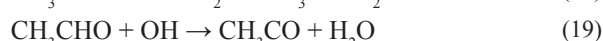
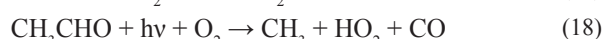
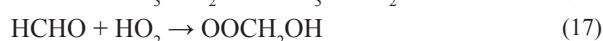
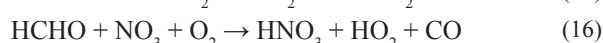
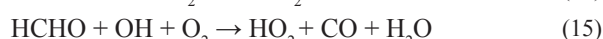
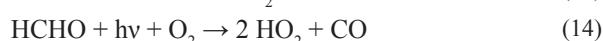
HO₂ and NO₂ makes several interactions with others compound present at the air, resulting on addition of nitric acid to the atmosphere (03). HNO₃ is the main product of the NO_x oxidation and have average concentrations in order of 5×10⁻⁵ ppm in urban areas (Kanaya *et al.*, 2007). The photolysis of NO₂ increases the molecular oxygen (O) concentration, a highly reactive specie that reacts with free oxygen in the air to produce ozone.



Once formed, ozone begins its cycle reacting chemically with NO (06), HO₂ (07) and OH (08), and realizing photolysis processes (09 and 10) when exposed to solar radiation with wavelengths less than 319 nm. The sequence of reactions and photolysis does not result in any chain reactions effect, but produces a highly energy and reactive specie called excited oxygen molecule (O (¹D)). This molecule collides with gases such as nitrogen (N₂) and oxygen (O₂), loses energy and returns to normal form (11 and 12) which reacts with O₂ again to produce ozone.



Recent studies about air quality monitoring in Rio de Janeiro city shows a high correlation between increased VOCs concentrations and growing CNG automotive fleet. The high emissions of CNG-fueled vehicles are directly linked to inadequate process of cars adaptation to use this kind of alternative fuel (Martins & Arbilla, 2003). According to Hsieh & Tsai (2003), formaldehyde represents 5-7% of total VOC concentration in urban atmosphere, while acetaldehyde represents 3-5%. Together, these aldehydes can reach 12% of total VOC's concentration. Both pollutants are directly emitted and chemically produced in the atmosphere. There are four possible facts for reactions involving aldehydes in an urban atmosphere: reactions with OH, HO₂, NO₃ and the photolysis process (Martins & Arbilla, 2003).



Nitric acid (HNO₃) formed from (16) and (20) does not generate large concentrations when compared with the production on reaction (03). The specie OCH₂OH formed at (18) represents a possible formation of peroxyacetyl nitrate (PAN), an important pollutant of urban atmosphere due to its damage to human health as a possible carcinogen and as an eye and lung irritant (Ginnebaug *et al.*, 2010). The acetyl radical (CH₃CO), product of (19) and (20), is used to acetaldehyde formation. The reactions above shows production of HO₂ and CO, and also the methyl radical (CH₃) which may be oxidized to form HCHO. Note that reaction between CH₃CHO and HO₂ was not considered because it's occurs with low frequency in atmospheric environment.

2.2 Chemical Kinetics

The study of concentration behavior for atmospheric chemical species follows the Law

of Guldberg-Waage, also known as Law of Mass Action, which says: For an elementary stage (21) related to a mechanism of chemical reactions, the Law of Mass Action order is given by stoichiometric coefficient of the species itself.



$$\frac{d[A]}{dt} = -k_{21}[A]^a[B]^b \quad (22)$$

where [A] and [B] are the concentration values ($molecule.cm^{-3}$) of consumed species in the atmosphere by reaction (21), [C] and [D] are the concentration values ($molecule.cm^{-3}$) of produced species in the atmosphere by reaction (21), and k_{21} is the second-order rate coefficient ($cm^3.molecule^{-1}.s^{-1}$) which represents the speed that reaction (21) occurs. Chemical reactions are caused mainly by collision between particles and reagents, and the degree of agitation of these particles is critical in terms of energy for this reaction to occur. Therefore, some reactions are characterized by environmental temperature dependence (T). This relationship is described by the Arrhenius equation (Jacobson, 2005):

$$k_i = A e^{-E_a/RT} \quad (23)$$

where A is the pre-exponential constant (the contact area dependence, among others) and E_a is the activation energy (both parameters are characteristic of each reaction and are obtained experimentally), R is the ideal gas constant, and T_k is the air temperature in Kelvin scale.

In the atmosphere, beyond reactions between molecules, there are also reactions named of photochemical, where the molecule undergoes in a process of photolysis when exposed to solar radiation at a given wavelength (also constitutes a feature of the reaction). Thus, by convention, these reactions receive other notation to rate coefficient: the photolysis rate j_i , which indicates a reaction as photochemical.

Table 1 summarizes the rate coefficients (k_i) and photolysis of the atmospheric photochemistry system used in this work. Each k_i are indexed by the reaction number. All these rate coefficients derive from Arrhenius equation with results in $cm^3.molecule^{-1}.s^{-1}$ as presented by Sander *et al.* (2003). Note that almost all k_i have air temperature dependence, except k_{11} and k_{12} , and k_{01} which have atmospheric pressure

| | | |
|----------|--|----------------------------|
| k_{01} | = $1.50 \times 10^{-13} (1 + 0.6(P_{atm}/1000))$ | Sander et al. (2003) |
| k_{02} | = $3.50 \times 10^{-12} \exp(250/T_k)$ | Sander et al. (2003) |
| k_{03} | = $2.50 \times 10^{-11} (T_k/300)$ | Sander et al. (2003) |
| j_{04} | = TUV model (reaction 4) | Madronich (1993) |
| k_{06} | = $3.00 \times 10^{-12} \exp(-1500/T_k)$ | Sander et al. (2003) |
| k_{07} | = $1.00 \times 10^{-14} \exp(-490/T_k)$ | Sander et al. (2003) |
| k_{08} | = $1.70 \times 10^{-12} \exp(-940/T_k)$ | Sander et al. (2003) |
| j_{09} | = TUV model (reaction 3) | Madronich (1993) |
| j_{10} | = TUV model (reaction 2) | Madronich (1993) |
| k_{11} | = 1.80×10^{-11} (no T_k dependence) | Sander et al. (2003) |
| k_{12} | = 2.20×10^{-11} (no T_k dependence) | Sander et al. (2003) |
| j_{13} | = TUV model (reaction 16) | Madronich (1993) |
| j_{14} | = TUV model (reaction 16) | Madronich (1993) |
| k_{15} | = $9.52 \times 10^{-18} \exp(2.03 \times \log(T_k) + (636/T_k))$ | Von Kuhlmann et al. (2006) |
| k_{16} | = $3.40 \times 10^{-13} \exp(-1900/T_k)$ | Sander et al. (2003) |
| k_{17} | = $6.70 \times 10^{-15} \exp(600/T_k)$ | Sander et al. (2003) |
| j_{18} | = $0.19 \times j_{13}$ | Sander et al. (2003) |
| k_{19} | = $5.60 \times 10^{-12} \exp(270/T_k)$ | Sander et al. (2003) |
| k_{20} | = $1.40 \times 10^{-12} \times (-1900/T_k)$ | Sander et al. (2003) |

Table 1 Arrhenius equations to the chemical reactions proposed in $cm^3.molecule^{-1}.s^{-1}$. and their respective sources.

dependence. The rate coefficient for formaldehyde and hydroxyl radical reaction in oxygen presence (k_{15}) was used as von Kuhlmann & Lawrence (2006). The photolysis rates (j_i) has units of s^{-1} and were estimated in an external radiative transfer model, TUV (Tropospheric Ultraviolet-Visible Model), developed by US National Center for Atmospheric Research (Madronich, 1993).

2.3 Ordinary Differential Equations System

Known the rate coefficients of photochemical system, the time variations of concentration for each consumed species are written according to the Law of Mass Action:

The Pseudo-Steady-State Approximation (PSSA) were applied to hydroxyl radical [OH] (31), hydroperoxyl [HO₂] (32) and excited atomic oxygen [O(¹D)] (33), becoming these three ODE's to algebraic equations. Many chemical reactions involves very reactive intermediate species such as free radicals, which, as a result of their high reactivity, are consumed virtually as rapidly as they are formed and consequently exist in very low concentrations. The pseudo-steady-state approximation (PSSA) is a fundamental way of dealing with such reactive

$$\frac{d[\text{CO}]}{dt} = -k_{01}[\text{CO}][\text{OH}] + [\text{HCHO}](j_{13} + j_{14} + k_{15}[\text{OH}] + k_{16}[\text{NO}_3]) + j_{18}[\text{CH}_3\text{CHO}] \quad (24)$$

$$\frac{d[\text{NO}]}{dt} = j_{04}[\text{NO}_2] - [\text{NO}](k_{02}[\text{HO}_2] + k_{06}[\text{O}_3]) \quad (25)$$

$$\frac{d[\text{NO}_2]}{dt} = -[\text{NO}_2](k_{03}[\text{OH}] + j_{04}) + [\text{NO}](k_{06}[\text{O}_3] + k_{02}[\text{HO}_2]) \quad (26)$$

$$\frac{d[\text{NO}_3]}{dt} = -[\text{NO}_3](k_{16}[\text{HCHO}] + k_{20}[\text{CH}_3\text{CHO}]) \quad (27)$$

$$\frac{d[\text{CH}_3\text{CHO}]}{dt} = -[\text{CH}_3\text{CHO}](j_{18} + k_{19}[\text{OH}] + k_{20}[\text{NO}_3]) \quad (28)$$

$$\frac{d[\text{HCHO}]}{dt} = -[\text{HCHO}](j_{13} + j_{14} + k_{15}[\text{OH}] + k_{16}[\text{NO}_3] + k_{17}[\text{HO}_2]) \quad (29)$$

$$\frac{d[\text{O}_3]}{dt} = j_{04}[\text{NO}_2] - [\text{O}_3](k_{06}[\text{NO}] + k_{07}[\text{HO}_2] + k_{08}[\text{OH}] + j_{10}) + k_{11}[\text{O}(^1\text{D})][\text{M}] \quad (30)$$

$$[\text{OH}] = \frac{k_{12}[\text{O}(^1\text{D})][\text{H}_2\text{O}] + k_{07}[\text{O}_3][\text{HO}_2] + k_{02}[\text{HO}_2][\text{NO}]}{k_{01}[\text{CO}] + k_{03}[\text{NO}_2] + k_{08}[\text{O}_3] + k_{15}[\text{HCHO}] + k_{19}[\text{CH}_3\text{CHO}]} \quad (31)$$

$$[\text{HO}_2] = \frac{j_{18}[\text{CH}_3\text{CHO}] + [\text{OH}](k_{01}[\text{CO}] + k_{08}[\text{O}_3]) + [\text{HCHO}](2j_{14} + k_{15}[\text{OH}] + k_{16}[\text{NO}_3])}{k_{17}[\text{HCHO}] + k_{02}[\text{NO}] + k_{07}[\text{O}_3]} \quad (32)$$

$$[\text{O}(^1\text{D})] = \frac{j_{10}[\text{O}_3]}{k_{11}[\text{M}] + k_{12}[\text{H}_2\text{O}]} \quad (33)$$

intermediates when deriving the overall rate of a chemical reaction mechanism (Seinfeld & Pandis, 2006). Therefore, the present system of equations is described by seven ordinary differential equations (24-30) and three algebraic equations (31-33), and all these 10 equations needs to be solved coupled.

3 Methodology

An empirical kinetic modeling approach was developed using box models concept to evaluate ozone, formaldehyde and acetaldehyde concentrations for an urban downtown area with high vehicular traffic. This kind of model represents a well-mixed parcel of air that can accommodate both seasonal and diurnal variations in emissions (Utembe *et al.*, 2005; Grant *et al.*, 2010).

3.1 Computational Modelling

The solution to equation system presented before falls in an initial value problem (IVP) described by a system of ordinary differential equations (ODEs) coupled. In other words, these equations must be solved simultaneously. Thus, to

obtain such a solution, a mathematical model was developed in FORTRAN 90 programming language, where the kinetic equations of ozone formation described above were implemented.

To solve this IVP in FORTRAN 90, the IMSL (Index Mathematical and Statistical Library) provides several subroutines to the most different characteristics of equations, for example, IVPRK (Initial Value Problem using Runge-Kutta), IVPAG (Initial Value Problem using Adams-Moulton or Gear) and DASPG (Differential-Algebraic System using Petzold-Gear). As the presented equation system has a stiff characteristic, the library does not recommend the subroutine IVPRK because it does not provide accurate solutions for this kind of problem. Also according to IMSL library the subroutine DASPG could be used, but this was developed for a very special case of matrix problems with terms equal to 1 or 0. Then, the most recommended is the subroutine IVPAG, which minimizes problems related to error propagation in numerical operations. This subroutine provides two different mathematical methods to solve equation systems: Adams-Moulton and Gear. Here, the second was chosen because, according to the IMSL library, it is the most consistent method for solution of ODE stiff systems.

3.2 Simulation Cases

After implementation of model equations in FORTRAN 90, several simulations were done to estimate diurnal variations of pollutant concentrations in an urban atmosphere, where a large amount of species emitted from different anthropogenic and natural sources are interacting in the same environment. The period of 16 hours of each simulation were made considering 57 600 time steps, starting at 06:00AM and ending at 10:00PM. The program was developed to depend of three input data files only: 1) initial concentrations of each species in ppm, 2) hourly meteorological data of air temperature (°C), relative humidity (%) and atmospheric pressure (mbar), and 3) TUV model output file with information about photolysis of photochemical reactions. The efficiency analyses of model were done through temporal evolution of each pollutant concentration simulated, which were compared to behavior described in literature.

The first test will evaluate the impact of seasonality on ozone formation. In presented EDO system, rate coefficients of photochemical reactions (j_i) are responsible for bring seasonality information to the problem. As these rates have a directly dependence of radiation flux, the highest values are expected at summer months when the study region receives the largest amount of solar energy. As mentioned earlier, photolysis rates were simulated through TUV model with default settings, except to geographical location and date of the simulation. The selected point is in Rio de Janeiro city, centered on the latitude 22.54°S and longitude 43.12°W. The meteorological data were selected considering two arbitrary days to represent summer and winter in the city of selected point (Table 2).

A second test was done to evaluate the increase of ethanol and CNG vehicle fleet at Rio de Janeiro. The city observed an increase of 267 053 to 961 793 to all vehicles using Ethanol fuel between 2002 and 2012. To all vehicles using CNG as fuel, this increase was of 50 649 to 422 592 at same period (DETRAN, 2014). Thus, Table 3 presents initial concentration used as base case to both tests mentioned. The first three concentrations were observed in experiment conducted in Rio de Janeiro, where NO, NO₂ and O₃ are annual concentration averages to 2005 collected at air quality station in the center of city. Others specie concentrations are typical of metropolitan areas, according to literature. In this second test, beyond the base case, other four simulations were done increasing 2 and 5 times only the acetaldehyde and the formaldehyde initial concentration.

| Time | Arbitrary Summer Day | | | Arbitrary Winter Day | | |
|----------|----------------------|----------|--------|----------------------|----------|--------|
| | T (°C) | P (mbar) | RH (%) | T (°C) | P (mbar) | RH (%) |
| 06:00 AM | 26 | 1010 | 88 | 17 | 1021 | 88 |
| 07:00 AM | 27 | 1010 | 85 | 17 | 1021 | 88 |
| 08:00 AM | 29 | 1010 | 79 | 19 | 1022 | 89 |
| 09:00 AM | 31 | 1010 | 74 | 19 | 1023 | 84 |
| 10:00 AM | 32 | 1009 | 69 | 21 | 1023 | 76 |
| 11:00 AM | 32 | 1009 | 69 | 23 | 1022 | 70 |
| 12:00 PM | 34 | 1008 | 65 | 23 | 1022 | 70 |
| 01:00 PM | 35 | 1007 | 60 | 24 | 1020 | 63 |
| 02:00 PM | 35 | 1006 | 63 | 24 | 1020 | 67 |
| 03:00 PM | 35 | 1005 | 66 | 23 | 1019 | 70 |
| 04:00 PM | 34 | 1004 | 68 | 23 | 1019 | 65 |
| 05:00 PM | 32 | 1004 | 72 | 22 | 1020 | 68 |
| 06:00 PM | 30 | 1006 | 77 | 21 | 1020 | 76 |
| 07:00 PM | 26 | 1005 | 96 | 21 | 1021 | 76 |
| 08:00 PM | 26 | 1006 | 92 | 20 | 1021 | 80 |
| 09:00 PM | 27 | 1006 | 89 | 20 | 1021 | 75 |
| 10:00 PM | 26 | 1006 | 92 | 20 | 1021 | 75 |

Table 2 Meteorological data of two arbitrary days selected to represent summer and winter in Rio de Janeiro city.

| Chemical species | Concentration | Source |
|--|---------------------------|--------------------------|
| Acetaldehyde (CH ₃ CHO) | 5.60×10 ⁻³ ppm | Martins & Arbilla (2003) |
| Carbon Monoxide (CO) | 1.7 ppm | Martins & Arbilla (2004) |
| Formaldehyde (HCHO) | 5.60×10 ⁻³ ppm | Martins & Arbilla (2005) |
| Hydroperoxide Radical (HO ₂) | 8.12×10 ⁻⁵ ppm | Jacobson (2005) |
| Nitrogen Monoxide (NO) | 8.39×10 ⁻² ppm | Carvalho (2006) |
| Nitrogen Dioxide (NO ₂) | 4.53×10 ⁻² ppm | Carvalho (2006) |
| Nitrate Radical (NO ₃) | 4.06×10 ⁻⁴ ppm | Jacobson (2005) |
| Ozone (O ₃) | 5.46×10 ⁻³ ppm | Carvalho (2006) |

Table 3 Initial concentrations used at base case in ppm units and sources, respectively.

An additional test was done to evaluate how the relation between initial concentrations of acetaldehyde and formaldehyde impacts on ozone concentrations. In this case, all initial concentrations were kept, except to CH₃CHO and HCHO. To avoid other influences, meteorological data were fixed on 26.5°C to air temperature, 1010mbar to atmospheric pressure and 88% to relative humidity. These

parameters have several impacts on rate coefficients and photolysis rates, besides the direct relation between relative humidity and water concentration (H_2O) that acts on $O(^1D)$ stabilization.

4 Results and Discussions

To understand the diurnal ozone concentration profile is fundamental observe its precursor pollutants behavior. In this work, the precursors considered on equations are basically NO_x (NO and NO_2) and VOCs (CH_3CHO and $HCHO$). The hydroxyl radical is the key to ozone tropospheric formation. Highly reactive, this radical has a short life in the atmosphere because rapidly reacts with other pollutants. Therefore, it is natural to observe a competition between VOC's and NO_x to react with OH . Environments with high concentrations of VOC's means that OH reacts mainly with VOC's, providing more radicals to ozone formation. When these concentrations are low, OH reacts preferentially with NO_x decreasing radical concentrations and retarding O_3 formation (Seinfeld & Pandis, 2006).

Figure 1A shows the diurnal profile of NO_x to summer (solid lines) and winter (dotted lines) times, with black lines to NO and gray lines to NO_2 . At first hours, the reaction between NO and O_3 (producing $NO_2 + O_2$) dominates decreasing NO and increasing NO_2 . Subsequently, NO formation overcomes their consumption, producing a new peak due growth of photolysis rate j_p , mastermind of the single term of NO production and NO_2 sink. This inverse behavior between NO and NO_2 concentrations were expected due literature results (Seinfeld & Pandis, 2006; Arbilla & Oliveira, 1999). The release of these species in the environment begins the process

of ozone formation, providing needed supplies to maintain their precursors. In the end of period, concentrations of NO and NO_2 tends steady-state at same time. On seasonality issue, NO and NO_2 inverse behavior were observed again, but this time, with greater discrepancy. See NO_2 concentrations between 5:00 and 6:00PM, the differences between summer and winter were greater than 20%, and to NO , these differences do not reached 10%.

Analyzing VOCs diurnal profiles (Figure 1B), the concentrations of its components are always decreasing during the day due to the fact that our system of reactions have been formulated just to observe the consumption of these pollutants, i.e., there are no production terms to acetaldehyde (black lines) and formaldehyde (gray lines). As expected, the $HCHO$ is abruptly consumed by reactions system, reaching steady-state in early afternoon with near zero concentrations. On the other hand, acetaldehyde is consumed in a milder form, reaching steady-state in late afternoon only, after 5:00PM. These results agree with Martins & Arbilla (2003), showing that the proposed model can well represent the behavior of these common pollutants in the atmosphere of Rio de Janeiro. Regarding seasonality, both VOC 's have a more intense consumption at summer months, representing a greater availability of free radicals in this atmosphere during these months and, showing why VOC 's are seen as responsible for maintenance precursor species of tropospheric ozone.

These evidences from NO_x and VOC's analyses explain the higher ozone concentrations to summer results presented on Figure 1C (solid line). Since NO_2 is intensively consumed providing a large amount of atomic oxygen (O) to form O_3 . And the reaction with NO that reduces O_3 concentrations only takes significant magnitude in late afternoon.

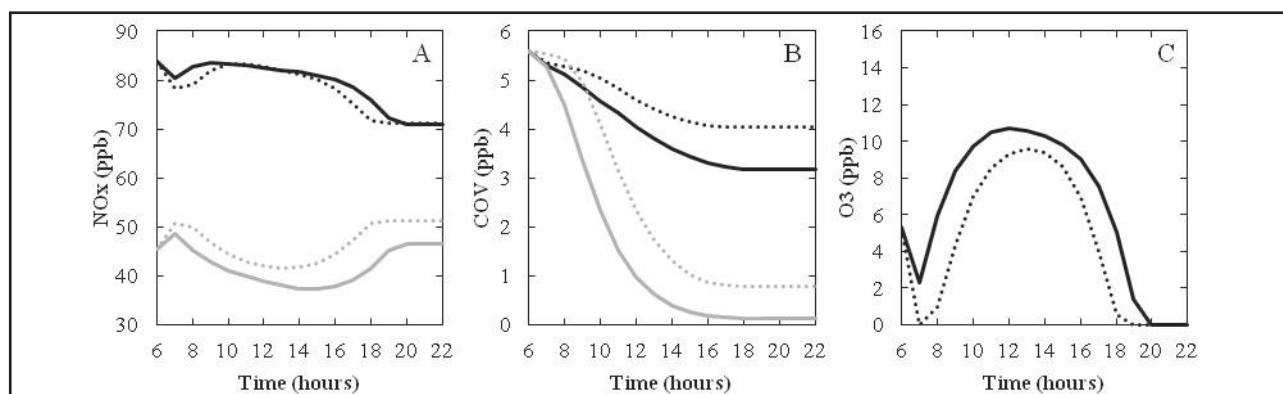


Figure 1 Diurnal variation of (A) NO_x , (B) COV, and (C) O_3 concentrations (ppb) to summer (solid line) and winter (dotted line) simulations. In Figure 1A, black lines represent NO concentrations and gray lines refer to NO_2 . In Figure 1B, black lines represent CH_3CHO concentrations and gray lines refer to $HCHO$.

Naturally, these peak levels were only possible due initial concentrations used to simulate an urban atmosphere. However, the proposed model proved to be able to simulate well these concentrations, showing that the main pollutant of photochemical smog reaches its peak between 2:00 and 3:00PM, agreeing with results reported in literature (Corrêa *et al.*, 2003; Machado *et al.*, 2000; Martins & Arbilla, 2003). Regarding seasonal variation, a significant difference were observed in ozone concentration between summer and winter simulations, reaching 20% at peak times as result of high photochemical activity of summer. Thus, summer months trends to be more propitious to kinetics of ozone formation than the winter months, agreeing with Ginnebaugh & Jacobson (2012).

Figure 2 presents simulated daily profiles to ozone concentration for different initial conditions of (A) nitrogen dioxides, (B) acetaldehyde and (C) formaldehyde. On Figure 1A, an increase of 1.5 and 2 times to NO_x initial concentrations provided a smooth elevation on O₃ levels when compared to the base case, with differences that did not exceed 2%. To simulation with NO_x increased 5 times, ozone concentration peak (12:00-2:00PM) reached 10% of base case concentrations. The same behavior was founded analyzing Figure 2B, the case of acetaldehyde increases. However, the most significant results were founded on cases with increases in formaldehyde initial concentration (Figure 1C), where ozone concentrations was 10% higher than the base case already in HCHO double increased simulation. Observing results of formaldehyde initial concentration 5 times increased, ozone levels exceed the base case close to 50%. This peak concentration is explained by high consumption of NO on reaction with HO₂ (O₂), which have its concentration elevated by HCHO consumption

on reactions 14, 15, and 16. Thus, decreasing NO concentration, the reaction 06 loses intensity and retard ozone consumption during the afternoon. This result shows the importance of control HCHO emissions due the growth of CNG vehicles fleet to prevent events such as photochemical smog.

To understand which VOC can produce higher ozone concentrations in proposed system of reactions, Figure 3 presents the O₃ diurnal peaks isopleths constructed varying CH₃CHO and HCHO initial concentrations. Note that fixing CH₃CHO initial concentration at 5 ppb, ozone peak concentrations increases ~20% varying HCHO initial concentrations from 10 to 20 ppb. Exchanging acetaldehyde for formaldehyde roles in this count, no significant increase can be observed on O₃ diurnal peaks, proving that increases on

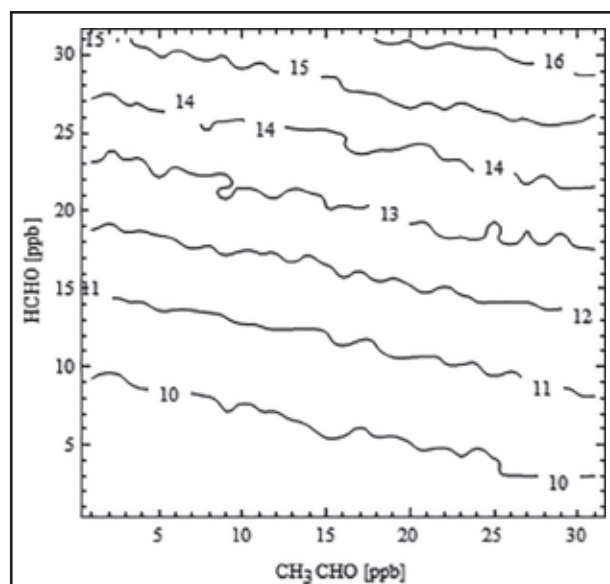


Figure 3 Ozone diurnal peaks isopleths (ppb) to different CH₃CHO and HCHO initial concentrations (ppb).

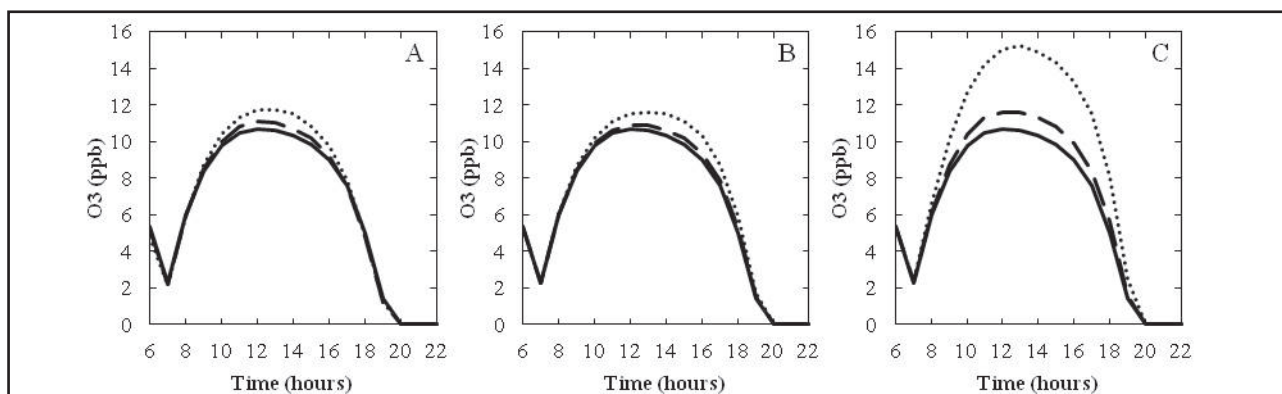


Figure 2 Diurnal variation of ozone (ppb) with an increase on initial concentrations of (A) NO_x, (B) Acetaldehyde, and (C) Formaldehyde. Solid lines represent the base case (equal to three simulations) and, dashed lines and dotted lines represents simulations with an increase of 2x and 5x on initial concentration of specific pollutant in base case, respectively.

HCHO emissions have more impacts on ozone formation than increases on CH₃CHO. The highest ozone peak concentration (~16 ppb) was found to cases with elevated acetaldehyde and formaldehyde initial concentrations. This result suggests that a combination of high CH₃CHO emissions with high HCHO emissions can improve substantially the tropospheric ozone formation.

5 Summary and Conclusions

A simplified mathematical model to kinetics of tropospheric ozone formation using FORTRAN 90 was developed and presented. The solution via DIVPAG subroutine proved to be consistent in represents a system of ordinary differential equations coupled with large differences on scales, case of atmospheric photochemical reactions. Simulation results showed a production/consumption behavior of pollutant concentrations according with expectations presented on literature. The evaluation of ozone concentrations to different seasons showed that summer months are more propitious to tropospheric O₃ formation in urban environment. The high intensiveness of photochemical reactions in this period was pointed as the main cause. Analysis of the influence of different initial concentrations showed alarming results for high emissions of formaldehyde, mainly provided from CNG fueled cars. As consequence, an elevation on ozone concentration levels was founded in peak hours (50% approximately), bringing up the question about the use of alternative fuels for vehicle fleets, the main source of the pollutants in the atmosphere.

6 References

- Anderson, L.G. 2009. Ethanol fuel use in Brazil: air quality impacts. *Energy & Environmental Science*, 2: 1015-1037.
- Arbilla, G. & Oliveira, K.M.P.G. 1999. Otimização de um mecanismo fotoquímico para a simulação da atmosfera urbana Brasileira. *Química Nova*, 22: 790-800.
- Assunção, J.V.; Pesquero, C.R.; Bruns, R.E. & Carvalho, L.R.F. 2005. Dioxins and furans in the atmosphere of Sao Paulo City, Brazil. *Chemosphere*, 58: 1391-1398.
- Corrêa, S.M. & Arbilla, G. 2005. Formaldehyde and acetaldehyde associated with the use of natural gas as a fuel for light vehicles. *Atmospheric Environment*, 39: 4513-4518.
- Corrêa, S.M.; Martins, E.M. & Arbilla, G. 2003. Formaldehyde and acetaldehyde in a high traffic street of Rio de Janeiro – Brazil. *Atmospheric Environment*, 37: 23-29.
- DETRAN. 2014. Departamento de Trânsito do Estado do Rio de Janeiro (<http://www.detran.rj.gov.br/>), website visited at June, 2014.
- Fornaro, A. & Gutz, I.G.R. 2003. Wet deposition and related atmospheric chemistry in the Sao Paulo metropolis, Brazil: part 2 - contribution of formic and acetic acids. *Atmospheric Environment*, 37(1): 117-128.
- Gaffney, J.S. & Marley, N.A. 1990. The search for clean alternative fuels: there's no such thing as a free lunch! *Atmospheric Environment*, Part A: General Topics 24.
- Gaffney, J.S. & Marley, N.A. 2009. The impacts of combustion emissions on air quality and climate – From coal to biofuels and beyond. *Atmospheric Environment*, 43: 23-36.
- Ginnebaugh, D.L. & Jacobson, M.Z. 2012. Examining the impacts of ethanol (E85) versus gasoline photochemical production of smog in a fog using near-explicit gas and aqueous chemistry mechanisms. *Environmental Research Letters*, 7(4): 1-8.
- Ginnebaugh, D.L.; Liang, J. & Jacobson, M.Z. 2010. Examining the temperature dependence of ethanol (E85) versus gasoline emissions on air pollution with a largely-explicit chemical mechanism. *Atmospheric Environment*, 44: 1192-1199.
- Graham, L.A.; Belisle, S.L. & Baas, C.L. 2008. Emissions from light duty gasoline vehicles operating on low blend ethanol gasoline and E85. *Atmospheric Environment*, 42: 4498-4516.
- Grant, A.; Archibald, A.T.; Cooke, M.C.; Nickless, G. & Shallcross, D.E. 2010. Modelling the oxidation of 15 VOCs to track yields of hydrogen. *Atmospheric Science Letters*, 11: 265-269.
- Grosjean, E.; Rasmussen, R.A. & Grosjean, D. 1998. Ambient levels of gas phase pollutants in Porto Alegre, Brazil. *Atmospheric Environment*, 32(20): 3371-3379.
- He, B.Q.; Shuai, S.J.; Wang, J.X. & He, H. 2003. The effect of ethanol blended diesel fuels on emissions from a diesel engine. *Atmospheric Environment*, 37(35): 4965-4971.
- Hsieh, C. C. & Tsai, J.H. 2005. VOC Concentration Characteristics in Southern Taiwan. *Chemosphere*, 50: 545-446.
- Jacobson, M.Z. 2005. *Fundamentals of Atmospheric Modeling*. Cambridge University Press, New York. 813 p.
- Kanaya, Y.; Tanimoto, H.; Matsumoto, J.; Furutani, H.; Hashimoto, S.; Komazaki, Y.; Tanaka, S.; Yokouchi, Y.; Kato, S.; Kajii, Y. & Akimoto, H. 2005. Diurnal variations in H₂O₂, O₃, PAN, HNO₃ and aldehyde concentrations and NO/NO₂ ratios at Rishiri Island, Japan: Potential influence from iodine chemistry. *Science of the Total Environment*, 376: 185-197.
- Knapp, K.T.; Stump, F.D. & Tejada, S.B. 1998. The effect of ethanol fuel on the emissions of vehicles over a wide range of temperatures. *Journal of the Air & Waste Management Association*, 48(7): 646-653.
- Machado, M.C.S.; Martins, E.M.; Corrêa, S.M. & Arbilla, G. 2000. Impacto do Uso de Combustíveis Oxigenados na Qualidade do Ar da Cidade de Rio de Janeiro. In: RIO OIL & GAS EXPO AND CONFERENCE, IBP26800.
- MacLean, H.L. & Lave, L.B. 2000. Environmental implications of alternative-fueled automobiles: air quality and greenhouse gas tradeoffs. *Environmental Science & Technology*, 34(2): 225e231.
- Madronich, S. 1993. UV radiation in the natural and perturbed atmosphere. In: TEVINI, M. (ed.). *UV-B radiation and ozone depletion. Effects on humans, animals, plants, microorganisms, and materials*. Lewis Publisher, p. 17-69.
- Martins, E. M. & Arbilla, G. 2003. Computer modeling study of

- ethanol and aldehyde reactivities in Rio de Janeiro urban air. *Atmospheric Environment*, 37: 1715-1722.
- Martins, E. M.; Arbilla, G.; Bauerfeldt, G. F. & De Paula, M. 2007. Atmospheric levels of aldehydes and BTEX and their relationship with vehicular fleet changes in Rio de Janeiro urban area. *Chemosphere*, 67: 2096-2103.
- Nguyen, H.T.; Takenaka, N.; Bandow, H.; Maeda, Y.; Oliva, S.T.; Boetelho, M.F. & Tavares, T.M. 2001. Atmospheric alcohols and aldehydes concentrations measured in Osaka, Japan and in Sao Paulo, Brazil. *Atmospheric Environment*, 25, 3075-3083.
- Sander, S.P.; Friedl, R.R.; Ravishankara, A.R.; Golden, D.M.; Kolb, C.E.; Kurylo, M.J.; Huie, R.E.; Orkin, V.L.; Molina, M.J.; Moortgat, G.K. & Finlayson-Pitts, B.J. 2003. Chemical Kinetics and Photochemical Data for use in atmospheric studies. *JPL Publication – NASA*, Evaluation Number 14.
- Seinfeld, J.H. & Pandis, S.N. 2006. *Atmospheric Chemistry and Physics of Air Pollution*. John Wiley & Sons, New Jersey, p1225.
- Tanner, R.L.; Miguel, A.H.; DE Andrade, J.B.; Gaffney, J.S. & Streit, G.E. 1988. Atmospheric chemistry of aldehydes: enhanced peroxyacetyl nitrate formation from ethanol-fueled vehicular emissions. *Environmental Science Technology*, 22: 1026-1034.
- Utembe, S.R.; Cooke, M.C.; Archibald, A.T.; Jenkin, M.E, Derwent, R.G. & Shallcross, D.E. 2010. Using a reduced Common Representative Intermediates (CRIv2-R5) mechanism to simulate tropospheric ozone in a 3D Lagrangian chemistry transport model. *Atmospheric Environment*, 44: 1609-1622.
- von Kuhlmann, R. & Lawrence, M.G. 2006. Supplementary material for Manuscript: The impact of ice uptake of HNO₃ on atmospheric chemistry. *Atmospheric Chemistry and Physics*, 6(1): 225-235.
- Wallner, T.; Miers, S.A. & McConnell, S. 2009. A comparison of ethanol and butanol as oxygenates using a direct-injection, spark-ignition engine. *Journal of Engineering for Gas Turbines and Power*, 131(3): 32802-32809.